CFRP ANCHORAGE SYSTEM FOR CFRP STRENGTHENED BEAMS

H. A. Rasheed[a*], B. R. Decker[b], A. Esmaeily[a], R. J. Peterman[a], H. G. Melhem[a]

[a]*Department of Civil Engineering, Kansas State University, 2118 Fiedler Hall, Manhattan, KS 66506*
[b]*Structural Design, Wallace Engineering, Colorado Springs, Colorado*
**hayder@ksu.edu*

Keywords: Anchorage System, CFRP Sheets, Flexural Strengthening, Concrete Beams.

Abstract

This research program is intended to verify the effectiveness of using external U-wrap CFRP distributed anchorage to increase the flexural strength contribution of externally bonded FRP composites. Premature FRP separation is a predominant failure mode in FRP flexural strengthening. Proper anchorage of flexural strengthening is anticipated to shift the failure mode from cover delamination or sheet debonding to a classical flexural failure by FRP rupture or concrete crushing. Once the cohesion of concrete and/or the adhesion with the FRP is exhausted, the U-wraps are engaged to provide anchorage to the flexural FRP through shear friction. Accordingly, three identical T beams and rectangular beams were designed and constructed to examine the capacity improvement by preventing premature debonding failure. The first specimen was tested as a control beam. The second specimen was strengthened using five layers of flexural CFRP only. The third specimen was strengthened with the same five layers of flexural CFRP plus additional transverse CFRP U-wrap stirrups. This study proved that it is possible to accomplish higher flexural capacity of CFRP strengthened beams using transverse CFRP stirrups.

1. Introduction

Structural strengthening and repair have become a major topic of interest over the past two decades due to the infrastructure needs for upgrades. Externally bonded Fiber Reinforced Polymer (FRP) provides a state-of-the-art technique for strengthening and rehabilitation. Traditional methods of strengthening involve the application of externally bonded steel plates. But some problems with this technique include the deterioration of bond between the steel and concrete due to steel corrosion, the difficulty to handle large steel plates and limited delivery lengths. Composites can provide a strengthening technique where the conventional systems do not work as efficiently. Specifically, FRP sheets can be used in place of steel plates. FRP sheets can be wrapped around a structural element to provide an increase in strength and ductility.

One drawback of the FRP flexural strengthening technique is the dominance of two premature failure modes, namely cover delamination and sheet debonding. These two modes alter the more classical flexural modes of FRP rupture and concrete crushing. While developing methods to predict cover delamination, several investigators formulated empirical and analytical expressions for that purpose [1-7]. Some of these procedures yielded inconsistent results [5, 7]. It was observed by other researchers that FRP debonding failure is still a dominant failure mode even in beams with FRP sheets extending close to the supports, where the stress concentrations are negligible [8-10]. To advance the performance of FRP strengthened beams, other studies focused on various ways to prevent such premature modes of failure, among which using different external end anchorage layouts [11-13].

The present study is intended to qualify the use of a distributed anchorage system to control both cover delamination and sheet debonding for beams more prone to those failure modes by virtue of having a considerable number of layers in flexural strengthening. T beams are examined to shift their failure mode to FRP rupture and rectangular beams are tested to shift their failure mode to concrete crushing.

2. Specimen Design

2.1. Beam Geometry

The beam design was performed using a nonlinear analysis program based on the incremental deformation technique. All of the beams have a length of 4877 mm with a clear span of 4724 mm. The T beams have a 152 x 305 mm web dimensions with the depth extending through the flange thickness, Figure 1(a). The flange dimensions are 406 mm width and 102 mm thickness. The main flexural reinforcement consists of 2 No. 5 bars. The compression steel consists of 4 No. 3 bars to hold the shear reinforcement caging Figure 1(a). The rectangular beams have a 152 mm x 305 mm cross section, Figure 1(b). The main flexural reinforcement is identical to that of the T section with 2 No. 3 bars used for the compression steel just to provide a caging framework for the shear reinforcement, Figure 1(b). Both the T and rectangular beams have shear reinforcement consisting of No. 3 stirrups at 127 mm on center, Figure 1(a-b). The complete dimensions of the two beam sections are listed in Table 1.

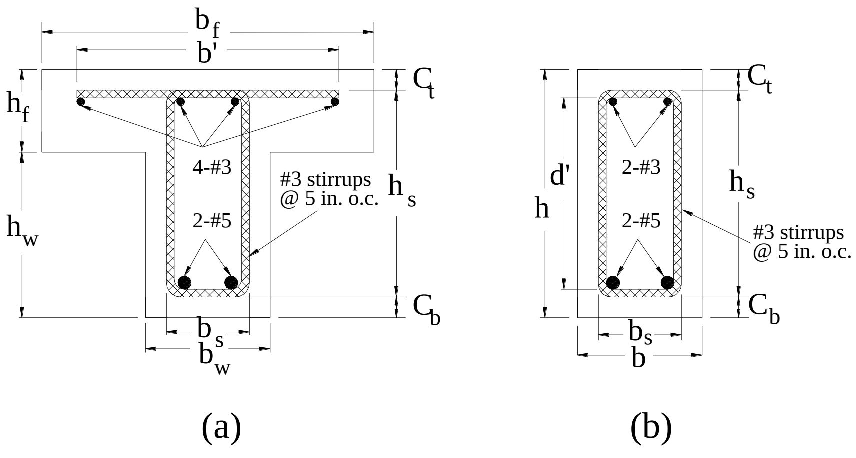

Figure 1 Beam Specimen Cross-Section (a) T-Beam (b) Rectangular Beam

2.2. Material Properties

The concrete that was used in casting the six beams is ready mix with a mix design nominal strength of 34.5 MPa. The average actual compressive strength of 18 test cylinders (102 x 203 mm) was 36.5 MPa. The material properties of the reinforcing steel were provided by the manufacturer to have a modulus of 200,000 MPa and yield strength of 483 MPa. The actual tensile testing of 3 samples of 8-inch long bar specimens was performed by KDOT research lab. The average modulus and yield strength of the No. 3 bars were 213,180 MPa and 450.6 MPa, respectively. The average modulus and yield strength of the No. 5 bars were 204,493 MPa and 480.45 MPa, respectively.

b_f	16 in (406.4 mm)
h_f	4 in (101.6 mm)
b_w	6 in (152.4 mm)
h_w	8 in (203.2 mm)
C_t	1 in (25.4 mm)
C_b	1 in (25.4 mm)
h_s	10 in (254 mm)
b’	13 in (330.2 mm)
b_s	4 in (101.6 mm)

Table 1 Dimensions of Beam Specimen Cross-Section

The material properties of the V-Wrap C100 High Strength Carbon Fiber Reinforced Polymer (CFRP) were provided by the manufacturer to have a modulus of 227,527 MPa, strength of 3792 MPa and sheet thickness of 0.165 mm based on the net fiber area. This corresponds to an ultimate strain of 0.017. The actual coupon tensile testing was performed based on ASTM Standard D3039. The modulus and strength averaged 59,931.6 MPa and 768.55 MPa based on the laminate area. These values were the average of 5 specimens as required by the ASTM Standard corresponding to an ultimate average strain of 0.0129.

3. Experimental Program

3.1. Test Setup and Data Acquisition

The flexural tests were performed in the structural testing lab of Kansas State University. The beams were loaded in four-point bending using a 1.22-m long steel spreader beam and a 222.5 kN hydraulic actuator. The actuator is controlled by a servo-hydraulic system called FlexTestGT from MTS system. The beams were simply supported with the supports placed 75 mm from the edge of the beam, providing a clear span of 4724 mm. Two-330 mm LVDT’s were placed on each side of the beam at mid-span.

3.2. Test Results

3.2.1 Control T Beam (T1)

The first specimen tested in the series of T-shaped beams is the control beam (T1). The beam was loaded in load control at a rate of 2.225 kN per minute. At a load of 48.95 kN, the system was switched to displacement control at a rate of 2.54 mm per minute. At first, the beam was predicted to fail at a load of approximately 54.8 kN. Flexural cracks began showing up at a load of approximately 19.1 kN. The beam failed at a load of 68.98 kN. Figure 2 shows beam T1 at the end of testing. Figure 3 shows the beam load-deflection response to failure. It is evident from Figure 3 that Beam T1 has a post-yield stiffness. This was incorporated in the refined analysis resulting in a failure load of 68.2 kN. At the failure load, the deflection at mid-span was 178 mm and the failure mode was concrete crushing in the flange at mid span, Figure 2.

Figure 2 Beam T1 at failure

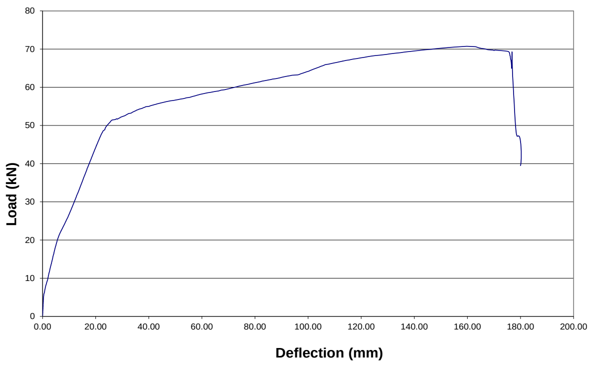

Figure 3 Load-deflection response of T1.

3.2.2 T-Beam with Flexural CFRP only (T2)

The next beam tested is the T-beam specimen with five layers of flexural CFRP reinforcement on the bottom surface of the beam in the longitudinal direction. For the test to be considered a success, the beam had to fail at a load higher than that of the control beam. Using the Teng et al model of predicting FRP debonding [10], it was estimated that the beam would fail at a load of approximately 117.9 kN. The beam was loaded in load control at the same load rate of 2.225 kN per minute. At a load of 66.75 kN, the control system was switched to displacement control at a rate of 2.54 mm per minute. The beam reached a load of 113.4 kN when the CFRP debonded with tremendous energy release. This failure load was very close to that predicted by Teng et al model. At the failure load, the deflection at mid-span was approximately 51 mm which is much smaller than the 178 mm deflection of the control beam. The CFRP detached with mostly debonding failure at the interface with small areas of concrete cover delamination shown in Figure 4. The load-deflection relationship for this beam specimen is shown in Figure 5.

Figure 4 Beam T2 at failure

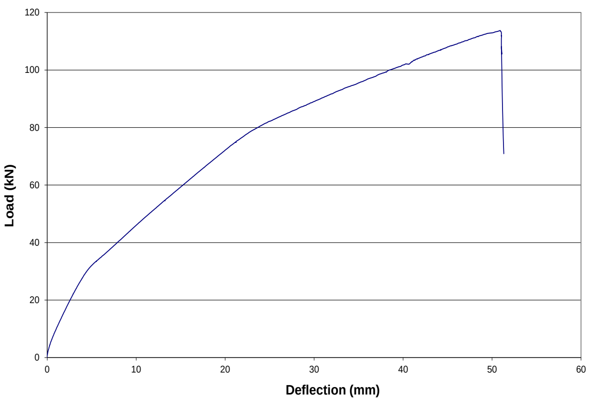

Figure 5 Load-deflection response of T2.

3.2.3 T-Beam with Flexural CFRP and U-Wrap Anchorage (T3)

The last beam tested in the series of T-beam specimens was strengthened with the same five layers of CFRP on the bottom surface of the web for flexural strength increase and it also had two layers of 127 mm wide U-shaped wraps around the web spaced at 305 mm on center. The purpose of these wraps was to anchor the bottom layers of CFRP in place as they tend to debond. This beam was loaded at the same rate of the previous specimens (i.e. 2.225kN per minute). The MTS system was programmed to switch to displacement control at a load of 160 kN. At a load of 116 kN, about the load at which separation occurred on beam T2, debonding of the flexural CFRP from the beam was seen in between the U-wraps. This was an excellent indication that the U-wraps were performing as they were supposed to by providing resistance to separation by shear friction. The beam reached an ultimate load of 149 kN when the CFRP ruptured, shown in Figure 6. The failure of this beam was more drastic than the previous beams since failure occurred prior to the system switching to displacement control. Figure 7 shows the load-deflection response of beam T3.

Figure 6 Beam T3 at failure

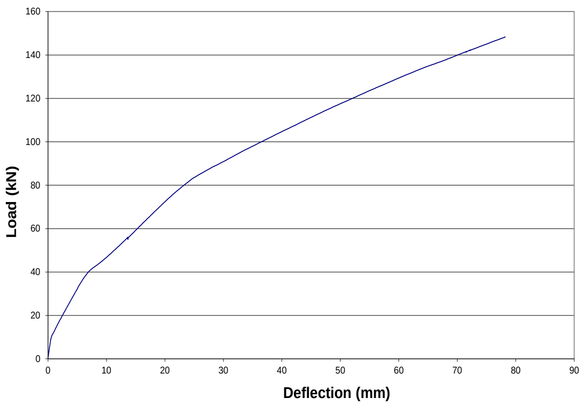

Figure 7 Load-deflection response of T3.

3.2.4 Control Rectangular Beam (R1)

The first beam tested in the series of rectangular beams is the control rectangular beam. It was determined from the flexural analysis program that the beam would fail at a load of 54 kN. The beam was loaded in load control at a rate of 2.225kN per minute. Cracking began taking place at a load of approximately 6.68 kN. At a load of 44.5 kN, the control system was switched to displacement control to capture the correct peak load. The rate of displacement was 2.54 mm per minute. The test results show that the beam failed at a load of 54.74 kN, which is very close to the theoretical value. The beam failed in a typical mode of steel yielding followed by crushing of concrete. Figure 8 shows beam R1 after failure and Figure 9 presents the load-deflection response of the beam.

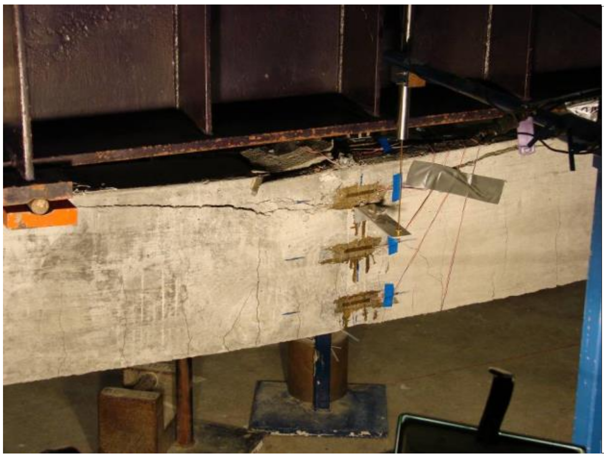

Figure 8 Beam R1 at failure

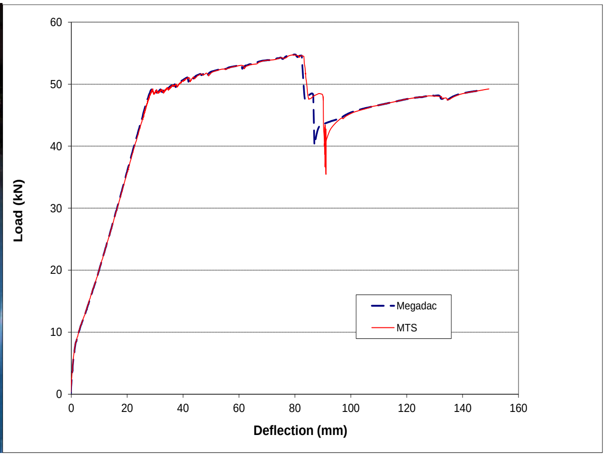

Figure 9 Load-deflection response of R1.

3.2.5 Rectangular Beam with CFRP Only (R2)

The next step was to strengthen the second rectangular beam with five layers of flexural CFRP sheets at the bottom face. For the test to be successful, delamination had to occur at a load higher than that of the control beam, which had an ultimate load of 54.74 kN. The CFRP was predicted to debond at a load of 91.23 kN using the Teng et al. debonding equation. The beam was loaded in load control at a rate of 2.225 kN per minute. At 53.4 kN, the system was programmed to switch to displacement control at a rate of 2.54 mm per minute. The load went well past that of the control beam. At a load of approximately 89 kN a lot of popping sounds started coming from the FRP which indicated the occurrence of local debonding. At a load of 109.4 kN, the CFRP reinforcement debonded/delaminated with tremendous energy release. This load was higher than that predicted by Teng et al. model, indicating a conservative approach in this case. The failure mode was mostly debonding failure between FRP and the concrete substrate as indicated by Figure 10. However, there were two small locations where the entire cover delaminated. Figure 11 shows the load-deflection results from this beam test.

Figure 10 Beam R2 at failure

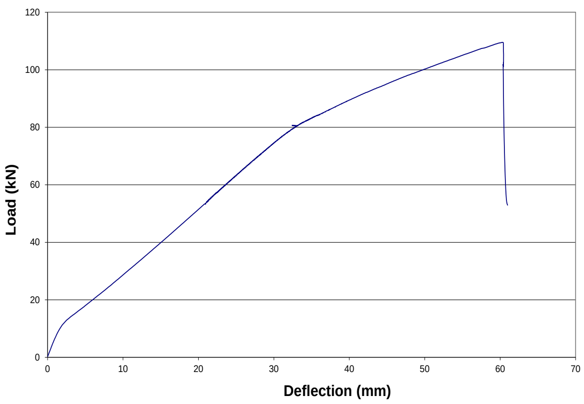

Figure 11 Load-deflection response of R2.

3.2.6 Rectangular Beam with CFRP and U-Wrap Anchorage (R3)

The last beam to test in the series of rectangular beams was the beam strengthened with the same five layers of CFRP on the soffit as beam R2 while this beam had one layer of 140 mm wide U-shaped wraps around the web spaced at 305 mm on center. The beam was loaded in load control at the same rate of the other beams. Once the test procedure was started, small cracking sounds were noticed around 26.7 kN, which seemed to be a sign of premature debonding. The noises continued throughout the test, but early debonding never occurred. At a load of 89 kN, the system was switched to displacement control. The load passed the magnitude of 109.5 kN, which is the ultimate debonding load from the previous test. This was an excellent indication that the U-wraps performed as they were supposed to by inducing resistance by shear friction once the resistance by cohesion is lost. The failure mode was initiated by the crushing of concrete cover. The beam reached an ultimate load of 120.5 kN when the CFRP ruptured, as shown in Figure 12. This load was slightly higher than the analysis value of 116.9 kN that was predicted to be associated with the concrete extreme compression fiber reaching a strain of 0.003. Figure 13 shows the load-deflection relationship that was obtained from this test.

Figure 12 Beam R3 at failure

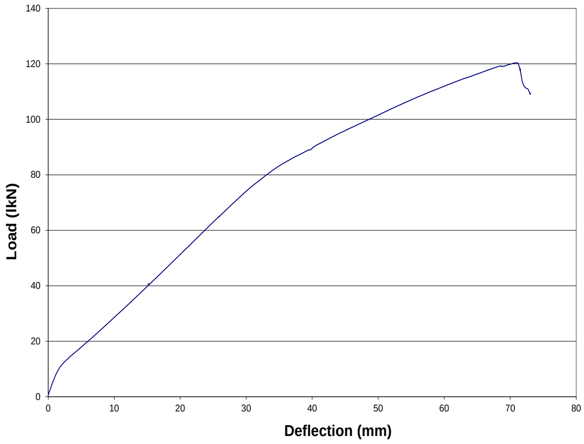

Figure 13 Load-deflection response of R3.

4. Numerical Analysis

4.1. Analysis Procedure

The incremental deformation technique for computing the moment-curvature response of the T and rectangular section is used, along with the integration of curvature along the beam, to generate the load-deflection response up to the full development of the classical sectional failure modes of concrete crushing or FRP rupture. The program is also capable of tracing the strains at different locations of the beam, which is beyond the scope of this paper.

4.2. Comparison with beam responses

The analysis procedure described above is used to compare the numerical response of beams T3 and R3 to the corresponding experimental response. Figure 14 and 15 show the close agreement between the test and analysis responses all the way to the ultimate load.

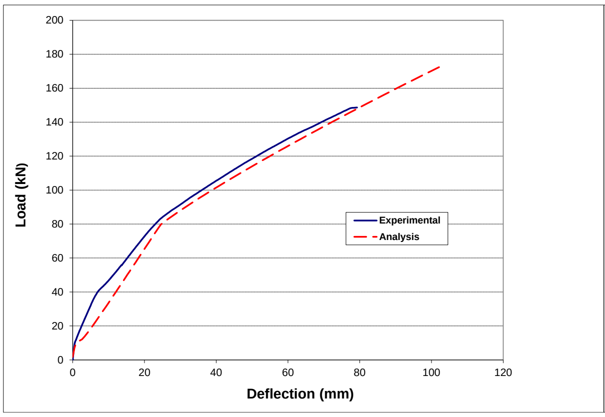

Figure 14 Comparison of test and analysis response of T3.

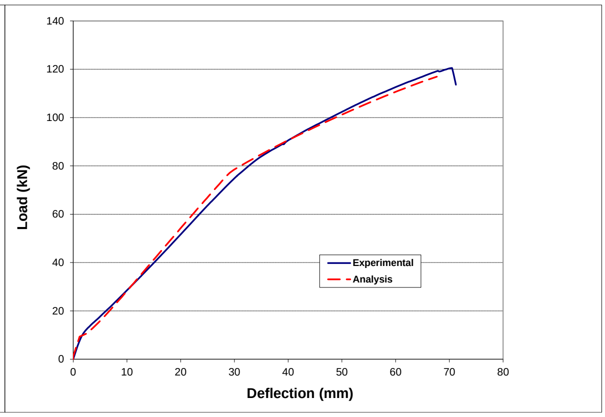

Figure 15 Comparison of test and analysis response of R3.

5. Conclusions

An experimental program is conducted to qualify the performance of a distributed CFRP anchorage system in controlling the deboning failure mode in T and rectangular beams leading to the attainment of the full flexural capacity. The results indicate the success of the technique in achieving its goals and the applicability of the Teng et al. model, implemented by the ACI 440.2R-08 [14], in conservatively predicting the debonding failure. The analysis program implemented is also shown to yield excellent correspondence to the overall experimental response.

References

[1] T. Roberts, "Approximate analysis of shear and normal stress concentrations in the adhesive layer of plated RC beams." *Struct. Eng.*, 67(12):228-233, 1989.

[2] R. Quantrill, L. Hollaway, and A. Thorne, "Predictions of the maximum plate end stresses of FRP strengthened beams: Part II." *Mag. Concrete Res.*, 48(177):343-351, 1996.

[3] B. Täljsten, "Strengthening of beams by plate bonding." *J. Mater. Civ. Eng.*, 9(4): 206-212, 1997.

[4] A. Malek, H. Saadatmanesh, and M. Ehsani, "Prediction of failure load of R/C beams strengthened with FRP plate due to stress concentration at the plate end." *ACI Struct. J.*, 95(2): 142-152, 1998.

[5] M. El-Mihilmy, and J. Tedesco, "Prediction of anchorage failure for reinforced concrete beams strengthened with fiber-reinforced polymer plates." *ACI Struct. J.*, 98(3): 301-314, 2001.

[6] H. A. Rasheed, and S. Perviaz, "Bond slip analysis of FRP strengthened beams." *J. Eng. Mech.*, ASCE, 128(1): 78-86, 2002.

[7] H. A. Rasheed, K. H. Larson and S. Nayyeri Amiri, "Analytical Solution of Interface Shear Stresses in Externally Bonded FRP-Strengthened Concrete Beams," *J. Eng. Mech.*, ASCE, 139(1): 18-28, 2013.

[8] C. Ross, D. Jerome, J. Tedesco, and M. Hughes, "Strengthening of reinforced concrete beams with externally bonded composite laminates," *ACI Struct. J.*, 96(2): 212-220, 1999.

[9] P. Fanning, and O. Kelly, "Ultimate response of RC beams strengthened with CFRP plates." *J. Compos. Constr.*, 5(2): 122-127, 2001.

[10] J. G. Teng, S. T. Smith, J. Yao, and J. F. Chen, "Intermediate crack-induced debonding in RC beams and slabs," *Constr. Build. Mater.*, 17(6-7), 447-462, 2003.

[11] A. Chahrour, and K. Soudki, "Flexural response of reinforced concrete beams strengthened with end-anchored partially bonded carbon fiber-reinforced polymer strips." *J. Compos. Constr.*, 9(2):170–177, 2005.

[12] F. Ceroni, M. Pecce, S. Matthys, and L. Taerwe, "Debonding strength and anchorage devices for reinforced concrete elements strengthened with FRP sheets." *Composites: Part B*, 39(3): 429–441, 2008.

[13] H. A. Rasheed, M. Nassajy, S. Al-Subaie, S. M. Abrishamchian, and A. Al-Tamimi, "Suppressing Delamination Failure Mode in Concrete Beams Strengthened with Short CFRP Laminates," *Mechanics of Advanced Materials and Structures*, 18(3): 194-200, 2011.

[14] ACI 440.2R-08, "Guide for the Design and Construction of Externally Bonded FRP Systems for Strengthening Concrete Structures," *ACI Committee 440*, Farmington Hills, MI, 76 p., 2008.